Irreversible Adsorption of an Aztec Dye on Fractal Surfaces

Ilich A. Ibarra, Sandra Loera, Humberto Laguna, Enrique Lima,* and Victor Lara

Universidad Autónoma Metropolitana, Iztapalapa, A. P. 55−532, Avenida San Rafael Atlixco No. 186 Col. Vicentina, 09340 México D.F., Mexico

Received June 10, 2005. Revised Manuscript Received August 15, 2005

Carminic acid was adsorbed into amorphous silicas prepared by the sol−gel process. While cromophore is gradually released in silica when put in contact with water, irreversible adsorption takes place when silica is doped with aluminum. The role of aluminum on effective retention of carminic acid by aluminic silicas is described. A fractal geometry approach was employed to describe changes in silica samples when they are doped with aluminum and when chromophore is incorporated. Inclusion of chromophore provokes aggregates to form interconnected fractal surfaces.

Introduction

Over the past decade, research has grown concerning dyes hosted in inorganic matrix. Indeed, the increasing studies on this subject are in response to the need of new materials, whose photophysical and photochemical properties could provide potential applications in the food, optical, electronic, and catalysis fields, among others.[1]

Several dye−inorganic matrix pairs have been synthesized successfully to be applied in very specific fields. In this sense, rhodamine B sulfo anchored at the walls of mesoporous MCM-41 was employed as SO_2 sensor.[2] Other examples are the azo dyes and phthalocianines encapsulated in the molecular sieves with the goal of using them as pigments.[3,4]

Recently, some works have reported the inclusion of carminic acid into inorganic materials, explaining its potential application in the food industry.[5,6] Works on this subject have achieved partial success, and other applications of these types of materials are limited because understanding of the inclusion of dye remains unclear. Furthermore, no reports have been given about the resistance to photodegradation of the molecule hosted in the matrix. Indeed, this dye, in pure form, it is sensitive to thermal degradation and photodegradation.

Carminic acid as pigment has been historically used by the Aztec race[7,8] who extracted the dye from the "cochineal beetle", an insect which lives on cactus plants. The Aztecs

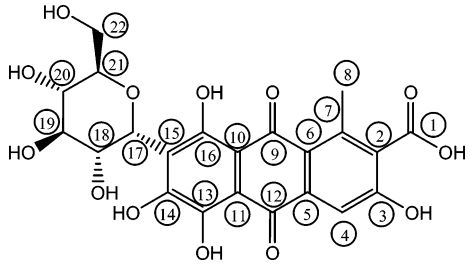

Figure 1. Molecular structure of carminic acid (*β*-D-glucopyranosyl-9,-10-dihydro-3,5,6,8-tetrahydroxy-1-methyl-9,10-dioxo-2-anthracenecarboxylic acid).

referred to carminic acid as *nocheztli*, which is a *nahuatl* word signifying "cactus blood".[9] During the conquest of Tenochtitlan (a city of the Aztec Empire), this dye was widely appreciated by the Spanish conquerors and then it was sent to Spain, where it was even used to dye the clothes of kings and to paint art pictures.[9−11] During the Industrial Revolution age, new pigments appeared and the use of *nocheztli* dye decreased significantly to the point of almost disappearing.

However, actually, many chemical pigments, especially those containing toxic metals have to be replaced, and the resurgence of organic dyes, such as carminic acid, Figure 1, takes place.

As mentioned above, there exist some reports about carminic acid in inorganic matrixes, such as silica, and they are mainly directed to use them as colorants in the food industry. However, the preparation method used until now for incorporation of carminic acid into silicas has been deposition in solution, which, surely, promotes only adsorption of the dye at the surface. It should be considered that the surface Si−O−Si−O bonds are exposed to hydrolysis; i.e., attack by water could result in leaching of the chromophore.

* Corresponding author. Telephone: (525) 55804 4667. Fax: (525) 55804 4666. E-mail: lima@xanum.uam.mx.

(1) Schulz-Eloff, G.; Wöhrle, D.; Van Duffel, B.; Schoonheydt, R. *Microporous Mesoporous Mater*. **2002**, *51*, 91.
(2) Ganschow, M.; Wark, M.; Wörle, D.; Schulz-Eloff, G. *Angew. Chem., Int. Ed*. **2000**, *39*, 161.
(3) Wark, M.; Ortlam, A.; Ganschow, M.; Schulz-Eloff, G.; Wörle, D. *J. Phys. Chem.* **1998**, *102*, 1548.
(4) Ganschow, M.; Wörle, D.; Schulz-Eloff, G. *J. Porphyrins Phthalocyanines* **1999**, *3*, 299.
(5) Díaz-Flores, L. L.; Pérez-Robles, J. F.; Vorobiev, P.; Horley, P. P.; Zakharchenko, R. V.; González-Hernández, J.; Vorobiev, Yu. V. *Inorg. Mater*. **2003**, *39*, 631.
(6) Atun, G.; Hisarli, G. *Chem. Eng. J*. **2003**, *95*, 241.
(7) Clendinnen, J. *Aztecs an Interpretation*; Cambridge University Press: Cambridge, U.K., 1995; p 243.
(8) Portillo, L.; Vigueras, A. L.; Flores, V. I. *Cria de Cochinilla*; Universidad Autónoma de Guadalajara: México, 2002; pp 1−3.
(9) Contreras, A. *Capital Comercial y Colorantes en la Nueva España, Segunda Mitad del Siglo XVIII*; El Colegio de Michoacán, Ed.; Universidad de Yucatán: México, 1996; pp 15−38.
(10) Zantwi, K. R. *The Aztec Arrangement*; University of Oklahoma Press: Norman, OK, 1985; pp 98−102.
(11) Wrigth, N. P. *Am. Dyes Rep.* **1963**, *52*, 53.

10.1021/cm051250n CCC: $30.25
Published on Web 10/22/2005

In this sense, soft conditions used in the sol−gel process[12] offer the advantage of incorporating chromophore in the synthesis step, and, then, occlusion of dye during cross-linking may be promoted.[13] The chromophore could bond to silanol groups or reach deep sites in the porous silica. Such functionalization or position of carminic acid in silica could inhibit its photodegradation or leaching, and then the hybrid system could find other applications, e.g. in the optical field. Indeed, carminic acid is interesting due to its potential application in tunable dye lasers and for decorative purposes. Such applications claim enhancement of lifetime, stability, and shielding of the dyes entrapped in the host materials.

On the basis of this subject, we started this work with the goal of finding a stable material containing carminic acid shielded from surface hydrolysis. For this, we propose to occlude the carminic acid during cross-linking reactions in the sol−gel process.

Experimental Methods

Materials. Glassy silica was synthesized by the sol−gel method. Tetraethoxysilane (TEOS) was used as the silicon source. TEOS was mixed with ethanol. An aging time of 96 h was elapsed, and then solvent was evaporated and the resulting solid dried at 100 °C; this sample was named G-Si. Silica doped with aluminum was obtained by adding the required amount of an aqueous solution of $Al(NO_3)_3$; The ratio Si:Al was 10:1, this sample was labeled as G-SiAl. Synthesis of G-Si and G-SiAl were repeated but carminic acid (CA), dissolved in ethanol, was added to the TEOS−ethanol mixture. Samples containing CA were referred to as G-Si(CA) and G-SiAl(CA), respectively. The content of CA in G-Si(CA) and G-SiAl(CA) samples was 11.3 and 10.1 wt %, respectively.

Carminic Acid Leaching. A 10 mg amount of sample containing CA was put in contact with 25 mL of water and then was shaken for 30 min. The leached amount of CA was quantified by ultraviolet−visible spectroscopy (UV−Vis).

Characterization. Materials were characterized by X-ray diffraction (XRD), small-angle X-ray scattering (SAXS), multinuclear solid-state nuclear magnetic resonance spectroscopy (NMR), and nitrogen adsorption/desorption at 77 K.

N_2 adsorption isotherms were determined at 77 K by a volumetric adsorption autosorb-1 quantachrome apparatus. Prior to adsorption of N_2, all the samples were outgassed at 120 °C for 12 h.

XRD patterns were collected on a Siemens D500 diffractometer using Cu Kα radiation.

The radial distribution functions (RDFs) were calculated from the full diffraction patterns as shown by Magini and Cabrini.[14] A molybdenum anode X-ray tube was used to reach the required high values of the angular parameter $h = (4\pi \sin \theta)/\lambda$ and the X-ray pattern was measured by step scanning at angular intervals of 0.08°.

A Kratky camera coupled to a copper anode tube was used to measure the SAXS curves. The distance between the sample and the linear proportional counter was 25 cm; a Ni filter selected the Cu Kα radiation. The sample was introduced into a capillary tube. Intensity $I(h)$ was measured for 9 min in order to obtain good-quality statistics.

The SAXS data were processed with the ITP program,[15−18] where the angular parameter (h) is defined as $h = 2\pi \sin \theta/\lambda$, where θ and λ are the X-ray scattering angle and the wavelength, respectively. The radius of gyration (R_g) could, then, be obtained from the slope of the Guinier plot, log $I(h)$ against h^2,[19] in the zone 1×10^{-3} Å$^{-2} < h^2 < 7 \times 10^{-3}$ Å^{-2}.

The shape of the scattering objects was estimated from the Kratky plot, i.e., $h^2I(h)$ against h. The shape is determined depending on the Kratky curve shape: for instance, if the curve presents a peak, the particles are globular.[20] If a shape can be assumed,[16] the size distribution function may be calculated.

Finally, it is often useful to estimate, from the slope of the curve log $I(h)$ vs log(h), the fractal dimension of the scattering objects.[21,22] The h interval was $0.07 < h < 0.18$ Å^{-1}.

Note that by the Babinet principle, the small-angle X-ray scattering may be due either to dense particles in a low-density environment or to pores or low-density inclusions in a continuous high electron density medium.

Solid-state NMR spectra were obtained under MAS conditions using an ASX 300 Bruker spectrometer with a magnetic field strength of 7.05 T, corresponding to a ^{27}Al Larmor frequency of 78.3 MHz. A single pulse method was used with a $\pi/2$ pulse of 2 μs and a recycle time of 0.5 s. The ^{27}Al chemical shift was referenced using an aqueous solution of $Al(NO_3)_3$ as external standard.

^{29}Si MAS NMR spectra were obtained operating the spectrometer at a resonance frequency of 59.59 MHz with a recycling time of 8 s and a pulse time of 3 μs. The spinning frequency was 5 kHz, and tetramethylsilane (TMS) was used as a reference.

^{13}C CP MAS NMR spectra were obtained at a frequency of 75.422 MHz using a 4 mm Cross-polarization (CP) MAS probe spinning at a rate of 5 kHz. Typical ^{13}C CP MAS NMR conditions for ^{1}H−^{13}C polarization experiment used a $\pi/2$ pulse of 4 μs, contact time of 1 ms delay time of 5 s, and 20 000 scans. Chemical shifts were referenced to solid shift at 38.2 ppm relative to TMS.

Results and Discussion

Structure. The X-ray powder diffraction patterns for four silica samples under study show amorphous materials, Figure 2. The diffractograms corresponding to crystalline carminic acid, also included in Figure 2, present diffraction peaks in two zones: the first one from 5 to 8 and the second one from 24 to 20 in the 2θ scale. However, when CA is incorporated into the silica network, the crystalline peaks fade out. Instead, a very broad line is observed. This suggests that the CA is occluded into amorphous material. This result is confirmed by the RDF results shown in Figure 3. Peaks are broad, not well-defined, confirming that no crystalline order is present. However, it is interesting to note one effect of introduction of aluminum in the silica: materials containing aluminum are less ordered, at long range, than the materials free of aluminum, as the peaks at distances larger than 0.5 nm are less defined.

(12) Pierre, A. C.; Elaloui, E.; Pjonk, G. M. *Langmuir* **1998**, *14*, 67.
(13) Levy, D.; Avnir, D. *J. Phys. Chem.* **1988**, *92*, 4731.
(14) Magini, M.; Cabrini, A. *J. Appl. Crystallogr.* **1972**, *29*, 702.
(15) Glatter, O. *J. Appl. Crystallogr.* **1981**, *14*, 101.
(16) Glatter, O. *J. Appl. Crystallogr.* **1984**, *17*, 435.
(17) Glatter, O. *Progress Colloid Polym. Sci.* **1991**, *84*, 46.
(18) Glatter, O.; Hainisch, B. *J. Appl. Crystallogr.* **1984**, *17*, 435.
(19) Kataoka, M.; Hagihara, Y.; Mihara, K.; Goto, Y.; Molten, J. *Mol. Biol.* **1993**, *229*, 591.
(20) Kataoka, M.; Flanagan, J. M.; Tokunaga, F.; Engelman, D. M. In *Use of X-ray Solution Scattering for Protein Folding Study in Synchrotron Radiation in the Biosciences;* Chanse, B., Deisenhofer, J., Ebashi, S., Goodhead, D. T., Huxley, H. E., Eds.; Clarendon Oxford Press: London, England, 1994; pp 4, 87−92.
(21) Harrison, A. *Fractals in Chemistry*; Oxford University Press Inc, New York, 1995.
(22) Shaefer, D.; Keefer, K. *Phys. Rev. Lett.* **1986**, *56*, 2199.

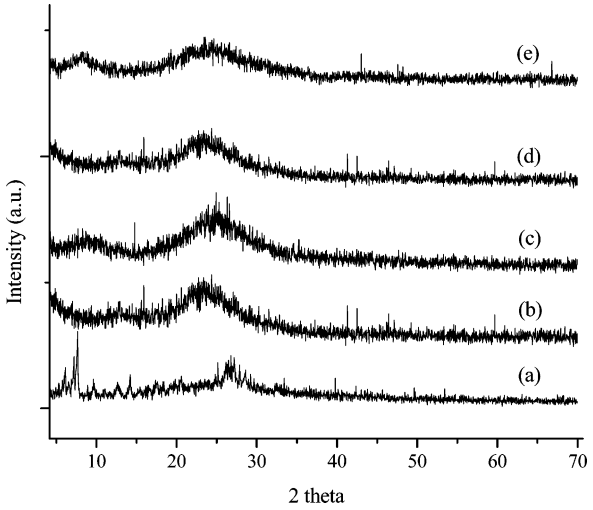

Figure 2. X-ray diffraction patterns of (a) carminic acid and silica samples: (b) G-Si, (c) G-SiAl, (d) G-Si(CA), and (e) G-SiAl(CA).

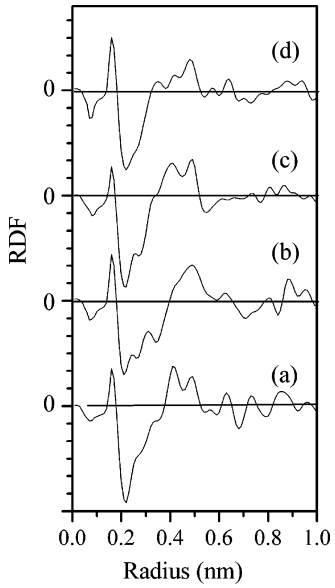

Figure 3. Radial distribution function of G-Si (a), G-SiAl (b), G-Si(CA) (c), and G-SiAl(CA) (d).

Table 1. Comparison of Interatomic Distances in Silica Samples Determined by the Radial Distribution Function

	interatomic distance (nm)				
sample	(Al,Si)−O	O−O	(Al,Si)−(Al,Si)	(Al,Si)−O	(Al,Si)−(Al,Si)
G-Si	0.162	0.259	0.331	0.406	0.489
G-SiAl	0.162	0.258	0.329	0.406	0.491
G-Si(CA)	0.162	0.257	0.330	0.406	0.491
G-SiAl(CA)	0.161	0.259	0.329	0.415	0.480

Table 1 compares the position of the first peaks in the RDF of samples under study. They are located at the same radial distances revealing similar interatomic distances in the first neighbors. This is not surprising as these distances correspond to the distances present in the primary units: tetrahedral composed of silicon−oxygen or octahedral composed of aluminum−oxygen.

As expected, the first three peaks are not modified in the samples containing carminic acid, as the carbon−oxygen distance is 0.157 nm. This value falls very close to distances corresponding to O−O or (Al,Si)−O, and therefore, it should not be resolved. Still, it is interesting to note a difference in the position of the peaks close to 0.41 and 0.48 nm in the

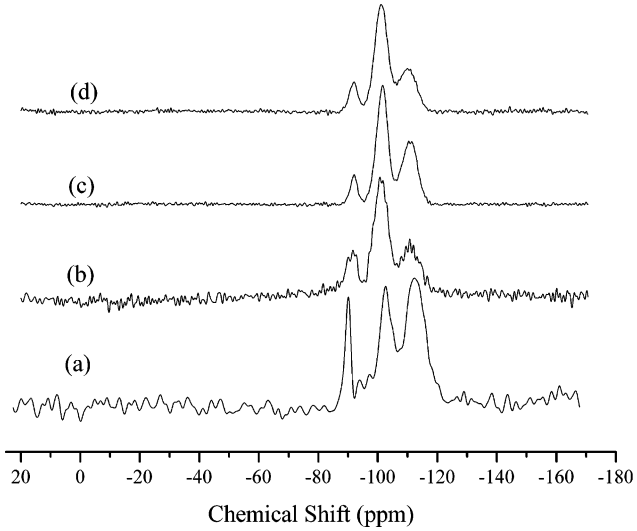

Figure 4. ^{29}Si MAS NMR spectra of G-Si (a), G-Si(CA) (b), G-SiAl (c), and G-SiAl(CA) (d).

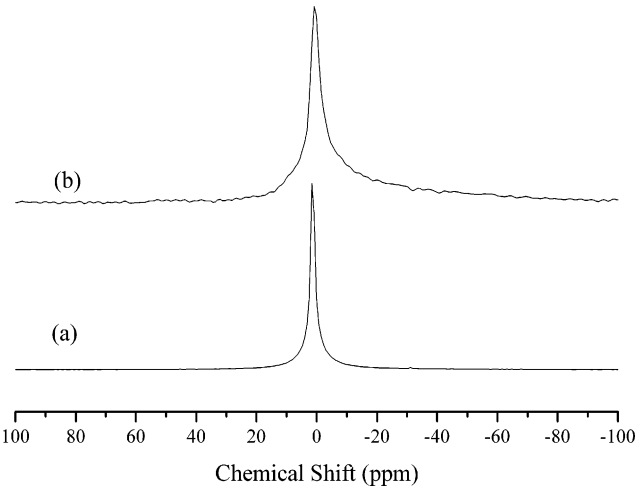

Figure 5. ^{27}Al MAS NMR spectra of G-SiAl (a) and G-SiAl(CA) (b).

RDF for samples containing carminic acid, G-Si(CA) and G-SiAl(CA). On one hand, the peak close to 0.41 nm may be due to the (Al,Si)−O distance (second neighbors), and it is therefore longer in the G-SiAl(CA) sample; on the other hand, the distance close to 0.48 nm may be due to (Al,Si)−(Al,Si), second neighbors, and it is therefore shorter in the G-SiAl(CA) sample. Then, surroundings of primary tetrahedral or octahedral units are altered by the presence of dye. The shortening and enlarging in the (Al,Si)−(Al,Si) and (Al,Si)−O distances in the dye-containing samples can be due to anchoring of carminic acid in the tetrahedral or octahedral units. In this sense, NMR results, Figures 4 and 5, can give more details about the dye−host arrangement. In silica, an oxygen of a silicon tetrahedron can either be a bridging oxygen (BO) or a nonbridging oxygen (NBO). BO are connected to another silicon tetrahedron and NBO are negatively charged and then nearby cation, e.g. a proton, acts as compensators of the charge. Nomenclature commonly used calls Q^4 units to silicon tetrahedral with their four oxygens being BO. Q^3 units contain three bridging oxygens and one NBO. Q^2, Q^1, and Q^0 units when the numbers of BO in the silicon tetrahedron are two, one, or zero, respectively. ^{29}Si NMR is used to identify the different Q units.[23]

Scheme 1

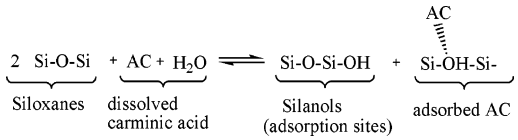

^{29}Si NMR spectra displayed in Figure 4 contain only three peaks close to −93, −101, and −109 ppm due to Q^2, Q^3, and Q^4 units, respectively, demonstrating that the frameworks are mainly composed of siloxane. The absence of the signals in the range from −50 to −60 ppm indicates that T units are not formed. T units correspond to R−Si species. The spectra included in Figure 4 should be compared taken in pairs. The first comparison is between the spectra corresponding to solids free of aluminum, G-Si and G-Si(CA) samples. In the G-Si sample there is, clearly, a higher amount of Q^4 units than in G-Si(CA) sample. By contrast the amount of Q^3 units is higher in G-Si(CA) than in G-Si sample. It seems that loading of CA inhibits the condensation reaction, $2Si{-}OH \rightarrow SiO{-}Si + H_2O$.

Indeed, as the time goes on during sol−gel synthesis, an aggregation of particles entraps solvent which changes its composition. The condensation from rich ethanol−aqueous solution changes to a water interface, and finally, through slow evaporation, only a few water molecules remain trapped. This change in the relative alcohol content is a consequence of the faster evaporation rate of alcohol, compared with a corresponding rate to water. Note that whereas the evaporation of ethanol stops quickly, the water is produced continuously by the reaction condensation. However, the addition of CA, which is soluble in water, may change the polarity of system network−solvent during the aggregation of particles as the reaction drawn in Scheme 1 may occur and it inhibits the condensation reaction.

The second comparison is between the samples doped with aluminum, which appear to have a different Q units distribution when they are loaded with or free of dye. Indeed, the intensity of the Si resonance in the Q^4 environment clearly decreases in sample loaded with CA. In contrast, intensity of Q^3 resonance augments. The following three Q^3 species could be formed in this material: $HO{-}Si{-}(OSi)_3$, $AlO{-}Si{-}(OSi)_3$, and $CA\text{-}O{-}Si{-}(OSi)_3$. Probably, $HO{-}Si{-}(OSi)_3$ are the species formed because, as shown below, CA seems to interact with aluminum species. CA−O−Al links could be promoted such that aluminum species or carminic acid loses protons which acidify the system, and, then, silanol groups appear, $HO{-}Si{-}(OSi)_3$. Thus, Q^3 units augment, and $Si{-}(OSi)_4$ species diminishes.

Interaction of CA with aluminum species is suggested from ^{27}Al NMR spectra, Figure 5. Note that aluminum does not change the coordination by introduction of dye. It is exclusively incorporated into silica as octahedral, with a signal close to 0 ppm,[24] Figure 5. Then, most probably, two types of layers are formed. The first layer is composed of tetrahedral SiO_4. Octahedral aluminum composes the second one. However, the ^{27}Al NMR peak in the spectrum of G-SiAl(CA) is broader and goes in 2 ppm toward stronger fields than in the corresponding signal of the sample G-SiAl. This result reveals a strong interaction of aluminum with oxygens or π orbitals from carminic acid. In this sense, the carbons interacting with aluminum should also alter their resonances as the ^{27}Al is a quadrupolar nucleus. ^{13}C CP/MAS NMR spectra displayed in Figure 6 and assignation[25] of peaks included in Table 2 show such alterations.

Comparing the spectra of solid CA and G-Si(CA) samples, minimal differences are observed in the position, width, and intensity of peaks. However, if the spectrum of solid CA is taken as reference, in the spectrum of G-SiAl(CA) the signals

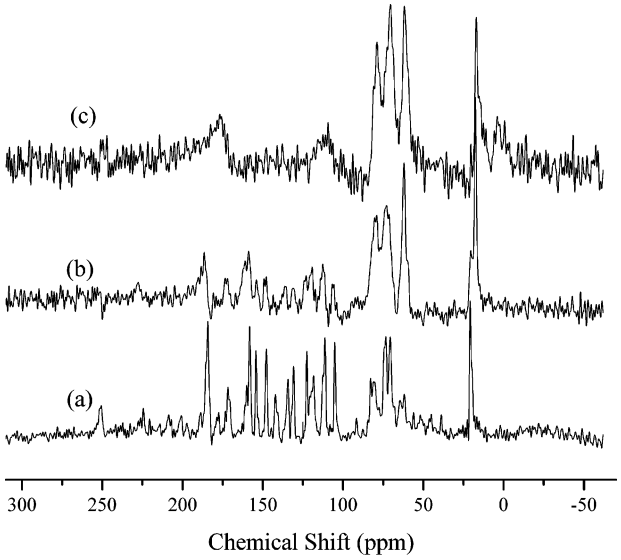

Figure 6. Solid-state ^{13}C CP/MAS NMR spectra of carminic acid (a), G-Si-(CA) (b), and G-SiAl(CA) (c).

Table 2. Attribution of ^{13}C NMR Peaks for Spectra Exhibited in Figure 6

	δ^a (ppm)		
carbon[b]	solid CA	G-Si(CA)	G-SiAl(CA)
1	171.73	172.30	N.O.
2	134.20	135.82	N.O.
3	157.60	158.79	N.O.
4	111.15	112.85	110.58
5	142.11	143.66	N.O.
6	123.00	123.53	110.58
7	142.11	143.66	N.O.
8	20.88	17.01	17.01
9	184.60	186.80	N.O.
10	105.00	106.70	110.58
11	111.15	112.85	110.58
12	184.60	186.80	176.70
13	148.20	147.00	N.O.
14	154.34	154.34	N.O.
15	118.43	119.60	110.58
16	159.92	161.60	N.O.
17	74.19	73.01	73.06
18	70.19	71.36	70.22
19	80.34	79.77	79.21
20	83.17	82.00	82.00
21	74.19	73.06	73.06
22	62.38	61.24	62.38

[a] δ = chemical shift. [b] Numbering of carbon atoms from Figure 1; N.O. indicates that the signal was not defined because of signal/noise ratio was very low.

(23) Melchior, M. T.; Vaughan, D. E. W.; Jacobson, A. J. *J. Am. Chem. Soc.* **1982**, *104*, 4859.
(24) Lippmaa, E.; Magi, M.; Samoson, A.; Engelhardt, G.; Grimmer, A. R. *J. Am. Chem. Soc.* **1980**, *102*, 4889.
(25) Kalinowski, H. O.; Berger, S.; Braun, S. *Carbon-13 NMR Spectroscopy*; John Wiley & Sons: New York, 1988.

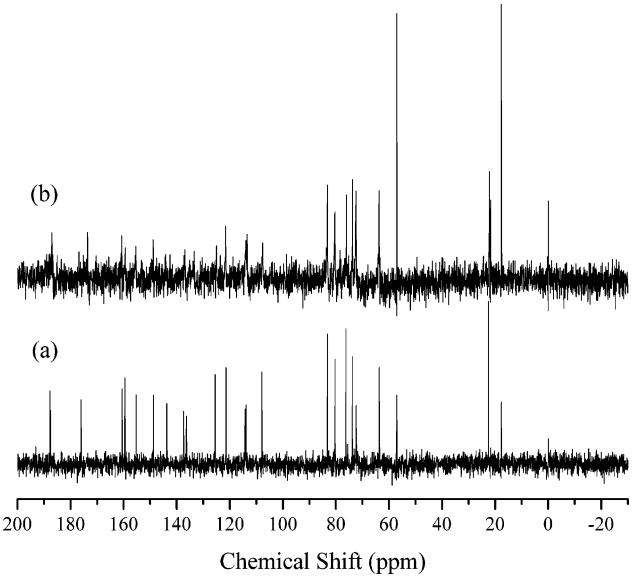

Figure 7. Spectrum ^{13}C CP/MAS NMR of carminic acid in liquid state dissolved in D_2O (a) and dissolved in D_2O containing Al^{3+} (b).

corresponding to aromatic and carbonyl carbons become very broad; even some resonances are difficult to observe because the signal/noise ratio is low. It is interesting to note that resonances of carbons from the glucose molecule (carbons 17−22) remain almost unaltered. It seems that in the G-Si-(CA) sample, the CA interact weakly with the SiO_2 matrix. In contrast, in the G-SiAl(CA) sample, aromatic and carbonyl carbons interact strongly with aluminum in the matrix. Solid-state NMR reveals such an interaction; however, it is not possible to give more details about this interaction because, in solid state, the observed NMR signals are often the nonisotropic peaks as they contain the effects of dipolar couplings or second-order effects which are not completely eliminated by spinning of the sample under MAS conditions.

Then, to confirm the interaction between aluminum and aromatic and carbonyl carbons, the following experiment was carried out: a solution containing carminic acid and aluminum was prepared, and, then, the ^{13}C CP/MAS NMR spectrum was recorded, Figure 7. The results were found to be similar to those reported in solids. The aromatic carbons appeared to be interacting strongly with aluminum and the peaks became broad. The following conclusion emerges: Carminic acid has a high affinity to bond to aluminum, probably to form a complex.

Morphology. Figure 8 compares the N_2 adsorption isotherms on G-Si and G-SiAl samples. The isotherm on G-Si belongs to type IV of the IUPAC classification,[26−28] where a hysteresis loop is observed and which is commonly associated with the presence of mesoporosity; the specific area was 406 m^2/g. The isotherm on G-SiAl presents an almost horizontal plateau over the range from 0.20 to 0.95 in the relative pressure scale. This isotherm approach to type

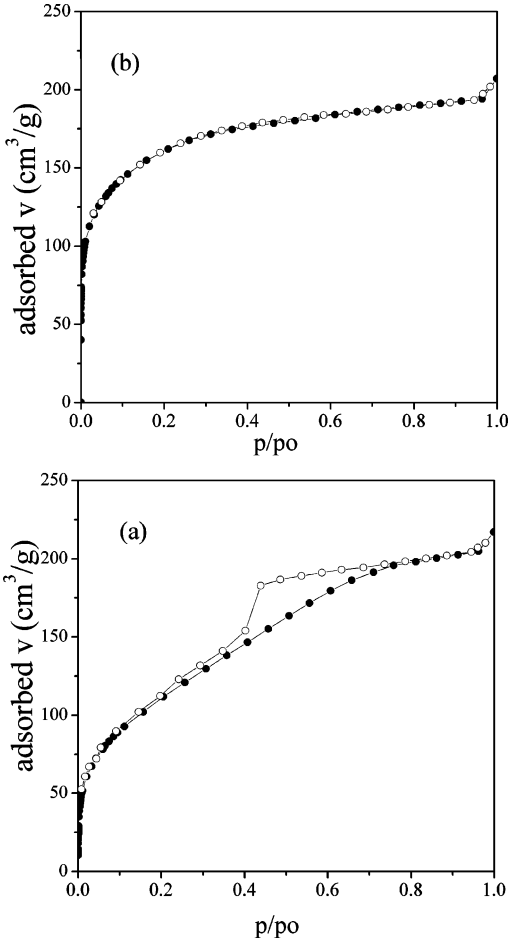

Figure 8. N_2 adsorption isotherms on samples G-Si (a) and G-SiAl (b), respectively: −●−, adsorption curve; −○−, desorption curve.

I, being characteristic of a microporous material, but as the sample sorbs N_2 at relative pressures higher than 0.20, it has to be concluded that also mesopores are present; the specific area for this sample was 713 m^2/g. Simply, the materials were synthesized by sol−gel, which is basically a polymerization−aggregation process. Undeniably during the process, initial polymerization produces small particles, which are connected through Si−O−Si bridges, and present Si−OH or Si−O− groups on the surface. With the introduction of aluminum during synthesis, the reactant system became acid and small particles coalesce to produce a network of fine particles entrapping some of solvent. As the solvent is removed, the cavities are formed and they depend, of course, on the characteristics of the primary particles and how they connected.

Dye containing samples were unable to adsorb N_2. Therefore, whereas aluminum enhances the developments of the microporous material, the dye inhibits the formation of open pores.

SAXS results indicate that the particles of four silica samples under study have a spherical shape, Figure 9. Assuming such shape, the particle size distributions were calculated; then a clear effect of the introduction of aluminum and carminic acid during synthesis of silica is observed, Figure 10. The term particles has to be understood in this work as the homogeneous microclusters. The size distribution of the sample G-Si is multimodal and present maximums at

(26) Brunauer, S.; Emmet, P. H.; Teller, E. *J. Am. Chem. Soc*. **1938**, *60*, 309.
(27) Brunauer, S. *The Adsorption of Gases and Vapors: Physical Adsorption*, Vol. I; Princenton University Press: Princenton, NJ, 1945.
(28) Sing, K. S. W.; Everett, D. H.; Haul, R. A.; Moscou, L.; Pieorotti, R. A.; Rouquerol, J.; Siemienniewska, T. *Pure Appl. Chem*. **1985**, *57*, 603.

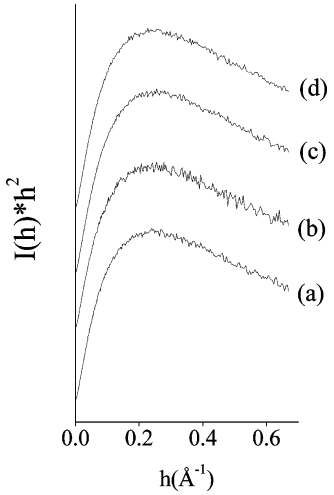

Figure 9. Kratky plots of the samples: G-Si (a), G-Si(CA) (b), G-SiAl (c), and G-SiAl(CA) (d). The shape of all curves corresponds to spheres.

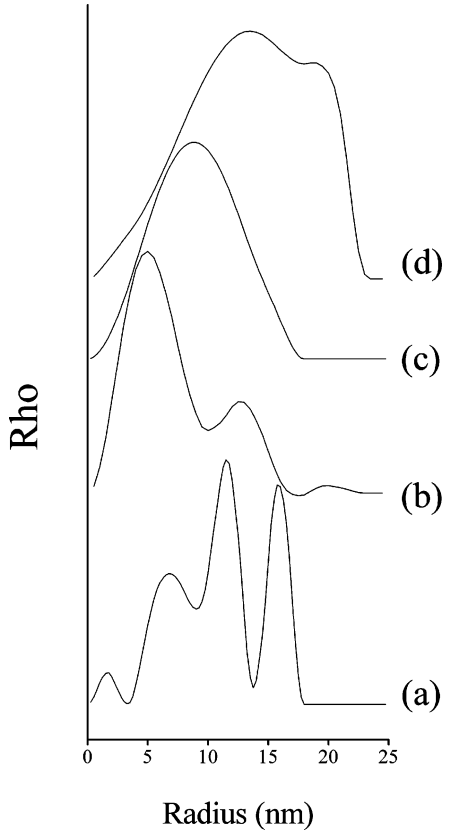

Figure 10. Particle size distributions in the following: G-Si (a), G-SiAl (b), G-SiAl(CA) (c), and G-Si(CA) (d).

1.4, 5.8, 11.5, and 16.4 nm. Note that the last two values are close to multiples of 5.8, and they suggest that the big particles are constituted by two or three smaller particles. A bimodal size distribution is observed for the sample G-SiAl with the mean peak at 5.0 nm, revealing that smaller particles are formed when aluminum is incorporated into silica. This is due to the coalescence of the fine particles as mentionated above. The size particle distribution is clearly altered when CA is added during the synthesis step; particularly a monomodal size distribution of big particles is favored. In G-SiAl (CA) a broad peak with maximum at 8.8 nm is observed, but since the peak is very broad, it has to be concluded that the size distribution is heterogeneous and

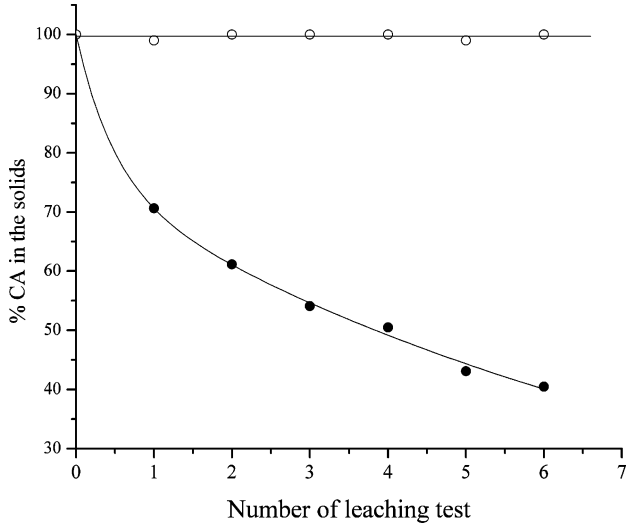

Figure 11. Carminic acid leaching from G-Si(CA) (−●−) and G-SiAl-(CA) (−○−), when samples were washed with water.

Table 3. Fractal Dimension of Silica Samples Determined from Slope of log *h* versus log *I*(*h*) Curves

sample	fractal dimension	sample	fractal dimension
G-Si	2.0	G-Si(CA)	2.9
G-SiAl	2.6	G-SiAl(CA)	2.8

particles with radii of 2.5 and 15 nm are present. Similar behavior is observed in the sample G-Si (CA); size particles are mainly distributed in the radius range from 7.6 to 21 nm. The growth of particles when CA is added suggests that the size of the structural primary units is significantly altered when the dye is present. Organic−inorganic hybrid units could form; when doing so they aggregate when the solvent is evaporated. In this sense, the fractal dimension, understood as the connectivity of the spheres, is most illustrative, Table 3. Sample G-Si has a fractal dimension $D = 2$, and this value augments when the sample is doped with aluminum and/or carminic acid. It reveals how the network is highly dense as the dye is incorporated into the amorphous material. During the synthesis of G-Si, the fractal aggregates appear to form a mass fractal of dimension 2. If the aluminum is added during the synthesis, as in the case of simple G-SiAl, then the aggregates occupy a larger fraction of the volume, leading to a larger fractal dimension indicative of a fairly irregular surface. Finally, in the solids containing carminic acid, fractal dimension values go close to 3, revealing an extreme irregularity of the surface.[29] Thus confirming that the density electronic is altered significantly at the surface because the carminic acid occupying some of surface of silica or doped aluminum silica. Note that fractal dimension is a morphological parameter and does not reflect the structural details emerged from NMR and DRX results. Furthermore, there are two solids which are porous, the G-Si and G-SiAl samples, where it is the backbone and not the pore space which is fractal; i.e., materials are constituted by interconnected fractal surfaces.

Carminic Acid Leaching. Figure 11 shows the curves of the amount of carminic acid retained in the G-Si (CA) and G-SiAl−(CA) samples after several leaching tests. A re-

(29) Avnir, D.; Farin, D. *Nature* **1984**, *308*, 261.

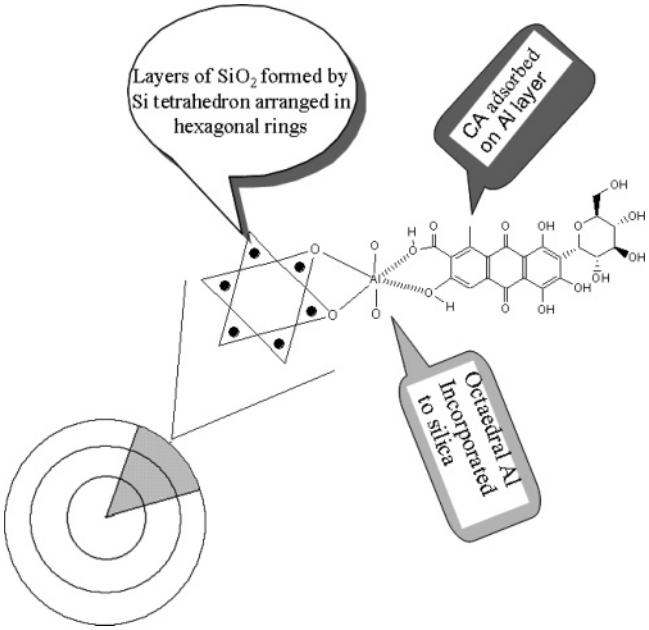

Figure 12. Representation of the adsorption of carminic acid on silica doped with aluminum. Zones indicated by unshaded, gray shaded, and black shaded boxes correspond to zones enriched in Si, Al, and CA, respectively.

markable stability of dye on the G-SiAl(CA) sample is observed as this sample does not leach CA after six leaching tests. On the contrary, the G-Si(CA) sample leaches gradually the dye, and after six leaching tests only 40% of the initial amount remains in the material. These results confirm a strong interaction between the aluminum and the carminic acid, as shown by the NMR results previously discussed. A model, at the molecular scale, for the irreversible adsorption of carminic acid in silica containing aluminum is represented in Figure 12.

Conclusion

Incorporation of carminic acid on amorphous silica during a sol−gel synthesis results in the creation of surfaces with irregularity in the electron density. The dye−silica materials may be described by interconnected silica fractals.

In carminic acid−silica material, the dye is weakly anchored to the surface, which is easily hydrolyzed, and as a consequence the dye leaches. In contrast, carminic acid incorporated into aluminum−doped silica, the organic molecule is strongly bonded to the aluminum−silica surface and remarkably stable even to hydrolysis.

Acknowledgment. The technical help of Alejandro Montesinos and Marco Antonio Vera (UAMI) is appreciated. Thanks to Richard Strager for help us.

CM051250N